Implementation of a P&O MPPT Algorithm in Low-Milliwatt-Scale Energy Harvesting Wireless Sensor Nodes

Kawsar Ali and Daniel J. Rogers
Department of Engineering Science
University of Oxford, OX1 3PJ, UK
Email: {kawsar.ali, dan.rogers}@eng.ox.ac.uk

***Abstract*—The Fractional Open-Circuit Voltage (FOCV) based Maximum Power Point Tracking (MPPT) method, typically used in low power energy harvesting circuits, is not truly dynamic and wastes harvestable energy in each MPPT cycle. Commercial-off-the-shelf (COTS) energy harvesting chips offer provision for externally setting the MPPT reference using more accurate and dynamic algorithms like Perturb-and-Observe (P&O), Incremental Conductance (INC) etc., but this can come at the cost of increased power consumption and sensing complexity. To address this issue, a simple low power implementation of the P&O method in an energy harvesting wireless sensor node (WSN) is presented in this paper. With only two additional analog load switches (SOT23 package), and no extra current or voltage sensor, the proposed method achieves dynamic MPPT with a power overhead of only eight microwatts.**

I. Introduction

On-board harvesting of ambient energy (light, heat, vibration, radio frequency signals etc.) complemented with a rechargeable energy storage (battery, supercapacitor etc.) has proven to be a competitive alternative to a traditional non-rechargeable-battery for powering wireless sensor nodes (WSN), by increasing their operating lifetime [1], [2]. For a given load power, the combined size of the energy harvester (EH) and rechargeable energy storage is minimised if maximum energy harvesting is ensured from the harvesters.

The maximum power point (MPP) of a source occurs where the product of their terminal voltage and output current is maximum. Energy harvesters like photovoltaic (PV) cells, thermoelectric generators (TEG) etc. are high output impedance sources. The method of extracting maximum power from such sources is called impedance matching or maximum power point tracking (MPPT). This is achieved with an active power-electronic circuit which dynamically controls the loading on the harvester to track its MPP. Depending on the environment parameters like temperature, irradiance etc., the MPP of a harvester may vary in a wide range. The MPPT method must be able to track this varying point efficiently.

Popular MPPT algorithms like Perturb-and-Observe (P&O) [3] and Incremental Conductance (INC) [4] use the sensed values of voltage and current of the harvester to compute its MPP. The analogue power management integrated circuits (PMICs) normally used in low power energy harvesting applications are not capable of doing such rather complex computation. Accurate sensing of harvester output current, which is often of the order of only microamperes, is another complexity to be addressed when implementing P&O and INC algorithms.

A simpler MPPT method, commonly found in many low power Commercial-off-the-shelf (COTS) energy harvesting PMICs, is the use of a constant voltage reference derived from the I-V characteristics of the harvester in its nominal operating condition. For example, in the LTC3105 [5], The MPP voltage is determined by

$$V_{\text{MPP}} = R_{\text{MPP}} \times 10^{-5} \tag{1}$$

where R_{MPP} is an external resistor. It is obvious that with the change of the harvester cell parameters due to external influence, this method may result in an operating point which is far away from the MPP. A better variant of this constant-voltage-reference approach, called the fractional open-circuit voltage (FOCV) method, is taken in many other PMICs [6]–[8], where the MPP voltage is determined by

$$V_{\text{MPP}} = kV_{\text{OC}}. \tag{2}$$

Here, k is a fraction set by a resistive divider and V_{OC} is the open-circuit voltage of the harvester. The value of k is usually set to 0.8 for PV cells and 0.5 for TEGs with the assumption that their MPP voltages are typically at about 80% and 50% of their open circuit voltages, respectively [9], [10]. In this method, the power drawn from the harvester is momentarily interrupted and the open-circuit voltage of the harvester is measured. The circuit then resumes operation with the harvester terminal voltage regulated at kV_{OC}. This is repeated in every MPPT cycle. While this technique is simple to implement and therefore suited for extreme low power harvesters (microwatts) where computational resources are limited, it wastes some harvestable energy during periodic V_{OC} sampling. This waste should, in theory, be avoidable as the harvester power increases (milliwatts and above) and more computational resource is available.

The FOCV method is also limited to the assumption of a fixed k value which, in reality, may change with varying operating conditions. For example, the choice of $k = 0.8$ is based on the standard test conditions (STC) of 1000 W/m² (one sun) of irradiance at an ambient temperature of 25°C. However, in practice, PV cell MPP voltage can vary in the

range 60% to 90% [11], [12] of the open-circuit voltage depending on the irradiance level and temperature, with the temperature effect being more pronounced.

To maximise the energy extracted from the harvester, a dynamic MPPT algorithm is desirable. Many COTS energy harvesting chips provide the option to externally set V_{MPP} from a microcontroller unit (MCU) using accurate dynamic algorithms like P&O or INC. However, the additional sensing requirement and the increased power consumption for maintaining a continuous MPP reference make this option less attractive.

This paper proposes a solution to this problem with an innovative and simple low power implementation of the P&O algorithm for an energy harvesting WSN. The on-board MCU, which is an integral part of a WSN (to drive the radio and read the sensor data), is used for the MPP computations. However, unlike the standard P&O implementation, the proposed method does not require sensing of the harvester voltage and current. Instead, it uses only the internal voltage sensor of the MCU to periodically sense the PMIC output voltage. Using this voltage, the average output power of the harvester is estimated and used in the P&O algorithm. No energy is wasted as the periodic sampling of harvester open-circuit voltage is avoided. The power overhead for implementing the proposed method is only a few microwatts.

II. System Description

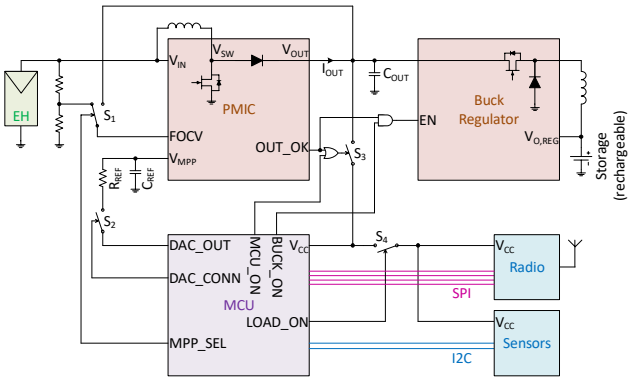

Fig. 1. Functional block diagram of the WSN with the proposed implementation of MPPT.

A simplified functional block diagram of the system is shown in Fig. 1. It is a standalone energy harvesting wireless sensor node comprising an energy harvester (EH), a power management integrated circuit (PMIC), a buck regulator, a rechargeable energy storage (supercapacitor), a microcontroller (MCU), a transceiver (radio), and an array of sensors. The radio and the sensors together are considered as the system load. In many cases, the buck regulator and the radio are integrated within the PMIC [7] and the MCU [13] respectively.

The PMIC boosts the input voltage V_{IN} into an unregulated output voltage V_{OUT} with a resistor-programmable upper bound $V_{\text{OUT,OV}}$. A bulk storage capacitor C_{OUT} is connected to V_{OUT} to accumulate enough energy to support the primary load of the system i.e. periodic sensing and radio transmission. Any excess energy from C_{OUT} is then passed on to the buck regulator which generates a regulated output voltage $V_{\text{O,REG}}$ which charges the supercapacitor. The body diode of the buck MOSFET helps to support the system load from the charged supercapacitor in the absence of input power from the harvester.

The OUT_OK signal from the PMIC indicates the state of V_{OUT}. It goes high when V_{OUT} surpasses V_{OKH} during the charging of C_{OUT}, and goes low when V_{OUT} falls below V_{OKL} during the discharging of C_{OUT}. The values of V_{OKH} and V_{OKL} are resistor-programmable. The logic OR and the logic AND gates shown in Fig. 1 helps the PMIC and the MCU in the overall operation and energy management of the system. This has been explained in detail in our previous work [14].

The FOCV MPPT [6]–[8] is implemented by periodically turning off the PMIC and then sampling the open-circuit voltage of the harvester. A fixed fraction (determined by the resistive divider) of this open-circuit voltage is used as the MPP reference voltage V_{MPP} and held in the capacitor C_{REF} during the period between two such sampling events. The PMIC, while on, simply tracks V_{MPP} to regulate its input voltage at the MPP.

To implement the proposed MCU-assisted MPPT method, we have introduced only two extra components – an SPDT switch S_1 and an SPST switch S_2. Switch S_1 is used for changing over from FOCV MPPT to MCU-assisted MPPT, and vice versa. Note that in MCU-assisted MPPT we disable the periodic sampling of the harvester open-circuit voltage (thus prevent wastage of harvestable energy), which is achieved by pulling up the FOCV pin to V_{OUT} in our system (see Fig. 1). Switch S_2 prevents the slow discharge of C_{REF} into the DAC_OUT pin of the MCU, after C_{REF} has been charged to V_{MPP}. A high value resistance R_{REF} ($\approx$10 MΩ) is used in series with C_{REF} to limit its charging current.

As common with low power WSN applications we make extensive use of the low power modes (LPM) [15], [16] of the MCU, where the central processing unit (CPU) and the individual peripherals can be turned-off selectively to minimize energy consumption when the MCU is sleeping. The roles of the general purpose input/output (GPIO) pins shown in Fig. 1 are summarised below.

- MCU_ON: is OR-ed with OUT_OK to keep the MCU on when $V_{\text{OKL}} > V_{\text{OUT}} > V_{\text{CC,MIN}}$. Here, $V_{\text{CC,MIN}}$ is the minimum supply voltage required for the MCU, which is typically 1.8 V. The MCU can be turned off only when both OUT_OK and MCU_ON goes low.
- BUCK_ON: is AND-ed with OUT_OK to ensure that the Buck regulator is disabled when $V_{\text{OKL}} > V_{\text{OUT}} > V_{\text{CC,MIN}}$, even if BUCK_ON is high. This prevents the sudden turn-off of the MCU during the trickle-charging cycles of the rechargeable storage (supercapacitor) on the buck regulator output bus ($V_{\text{O,REG}}$).
- LOAD_ON: controls the switch S_4 which is used for turning on/off the load (i.e. the radio and the sensors).

- MPP_SEL: controls the switch S_1 which is used for selection of MPPT mode between FOCV (MPP_SEL = 0) and MCU-assisted (MPP_SEL = 1).
- DAC_CONN: controls the switch S_2 which is used for making or breaking the connection between R_{REF} and the DAC_OUT pin.

III. Proposed Implementation of MPPT

A. Workflow in the System

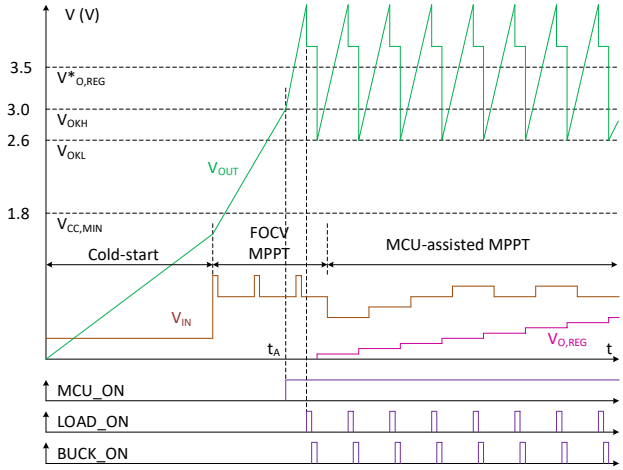

Fig. 2. Illustration of slow buildup of output voltages showing the transition from FOCV MPPT to the proposed MCU-assisted MPPT method. The time axis is not to scale..

Fig. 2 shows an illustration of the voltage build-up in the unregulated and the regulated output buses for our example case discussed later in section V. Note that the numeric values of different voltage levels in Fig. 2 are specific to this study, but the proposed method can be adopted to any other similar application as long as the following relation is satisfied.

$$V^*_{\text{O,REG}} > V_{\text{OKH}} > V_{\text{OKL}} > V_{\text{CC,MIN}}. \tag{3}$$

The major steps of the algorithm are described below.

1) The PMIC starts up in cold-start mode where all of its features are disabled except an auxiliary unregulated hysteretic boost converter whose only function is to charge up C_{OUT} to a minimum voltage required to power up the main boost converter [6].
2) The cold-start circuit is disabled when the main boost circuit is powered up. The output capacitor C_{OUT} is now charged by the main boost converter using FOCV MPPT method.
3) When the OUT_OK signal goes high for the first time (with $V_{\text{OUT}} = V_{\text{OKH}} = 3$ V at t_{A} in Fig. 2), the MCU is turned on, and it sets its MCU_ON signal high. Note that V_{CC} becomes equal to V_{OUT} after the turn-on of the MCU.
4) The MCU then goes to sleep (i.e. low power mode) for t_1 s. After waking up, the MCU checks if $V_{\text{CC}} > V^*_{\text{O,REG}}$.

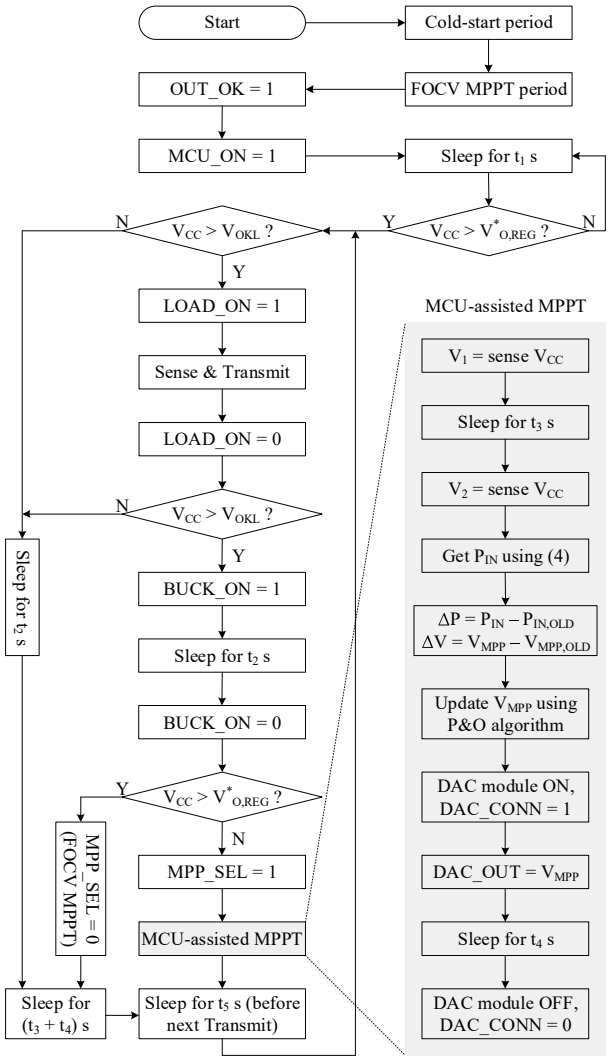

Fig. 3. Flowchart of proposed implementation of MPPT.

If not, it goes back to sleep again for t_1 s. This keeps on repeating until V_{CC} becomes greater than $V^*_{\text{O,REG}}$, when the MCU enters the infinite loop.

5) The infinite loop starts by ensuring $V_{\text{CC}} > V_{\text{OKL}}$. Since sensing and transmitting is the first priority of the system, the LOAD_ON signal is set high so that the radio and the sensors can perform their tasks. The LOAD_ON switch is pulled low when this is done.
6) If V_{CC} is still more than V_{OKL} after the radio transmission, the buck regulator is enabled by setting BUCK_ON signal high to charge the rechargeable energy storage (supercapacitor), and the MCU goes to sleep for t_2 s. The buck regulator is disabled when either V_{OUT} falls below V_{OKL}, or the MCU pulls the BUCK_ON signal low after waking up. This is taken care of by the logic AND operation between OUT_OK and BUCK_ON signals. The supercapacitor is thus trickle-charged in each

iteration.

7) At this point if $V_{\text{CC}} \leq V^*_{\text{O,REG}}$, the MPP_SEL signal is set high to enable the MCU assisted MPPT method, as described in the next subsection. However, if $V_{\text{CC}} > V^*_{\text{O,REG}}$, it is decided that the supercapacitor has been fully charged up to its target voltage $V^*_{\text{O,REG}}$ and the MPP_SEL signal is pulled low to fall back to the FOCV MPPT mode.
8) Finally, the MCU goes into another sleep period for t_5 s before going back to the next sense and transmit event (step 5).

Fig. 3 shows the flowchart of the proposed algorithm. It is easy to see that the system prioritises sense and transmit operation, and can continue to support it with energy from only the supercapacitor storage in the absence of harvester energy (e.g. at night for a PV-based WSN) until the supercapacitor voltage falls below V_{OKL}.

B. MCU-assisted MPPT

After the sense and transmit step (step 5) and the supercapacitor trickle-charge step (step 6) have been completed, the input energy from the harvester only charges the output capacitor C_{OUT}. Assuming the quiescent currents and leakage currents of various parts of the system as constant and negligible, the average input power is estimated as

$$P_{\text{IN}} = \frac{1}{\eta t_3} \int_{V_1}^{V_2} C_{\text{OUT}}(V) V . \mathrm{d}V \tag{4}$$

where V_1 and V_2 are the sensed values of V_{CC} (and therefore of V_{OUT}) using MCU internal voltage sensor with a fixed time interval t_3 between the two sensing events, and η is the nominal efficiency of the PMIC. Note that the value of C_{OUT} is a function of its dc bias voltage [17] since it is typically a class II (X7R, X5R etc.) ceramic capacitor. This function is estimated from the datasheet of the capacitor using a linear fit, as shown later in (6) for our example system.

The changes in input power and input reference voltage with respect to their previous iteration values are now calculated as

$$\Delta P = P_{\text{IN}} - P_{\text{IN,OLD}}.$$

$$\Delta V = V_{\text{MPP}} - V_{\text{MPP,OLD}}.$$

Using ΔP and ΔV from above equation a basic P&O algorithm is implemented [3] and the value of V_{MPP} is updated.

To charge C_{REF} to the updated V_{MPP} voltage, the DAC module of the MCU is enabled and the DAC_CONN signal is set high so that the DAC_OUT pin is connected to R_{REF}. The DAC_OUT pin is now held at V_{MPP} for t_4 s to complete the charging of C_{REF}. Once completed, the DAC_CONN signal is pulled low and the DAC module is disabled to save power.

Note that the switch S_2, which is connected between the DAC_OUT pin and R_{REF} and controlled by the DAC_CONN signal (see Fig. 1), is critical for this application to keep V_{MPP} steady for the duration between MPPT cycles, which is usually more than 10 s. The MCU pins typically have a leakage current of 50 nA even in their high-impedance state (tri-state). If the DAC_OUT pin is directly connected to R_{REF}, this leakage current can discharge C_{REF} (usually a few tens of nanofarads) within fraction of a second. The switch S_2 realised by a load switch with sub-nanoampere leakage current in its off-state (e.g. TPS22860) holds V_{MPP} at a steady value for several tens of seconds.

IV. Design Aspects

A. Output Capacitance

In the energy budget of the system, the sensing and radio transmission has the first priority, then any extra energy is used for charging the supercapacitor. Clearly, C_{OUT} has to be large enough to sustain at least one sense and transmission cycle [14], and therefore, is calculated as

$$C_{\text{OUT}} = I_{\text{LOAD}} t_{\text{LOAD}} / (V_{\text{OKH}} - V_{\text{OKL}}) \tag{5}$$

where t_{LOAD} is the combined duration of the sense and transmit events, and I_{LOAD} is the average current consumed by the load during t_{LOAD}.

For example, in our experiment described in the next section, we need a load current of 20 mA for a pulse duration of 40 ms. According to (5), for a V_{OKL} and V_{OKH} of 2.6 V and 3 V respectively, we need at least 2 mF of C_{OUT} to drive this load. Ceramic capacitors are generally preferred as C_{OUT} in low power WSN applications as they have very low leakage current. However, among the commercially available ceramic capacitors rated for voltage above 3 V, the highest capacitance value we could find is with the AMK432BJ477MM capacitor, rated as 470 µF, 4 V. Also, the effective value of capacitance of the class II ceramic capacitor (X7R, X5R etc.) drops drastically with the increase of dc bias [17]. We have used 10 numbers of AMK432BJ477MM capacitors in parallel. A simple linear fit of its dc bias characteristics from the datasheet is

$$C_{\text{OUT}}(V_{\text{X}}) = (-771 V_{\text{X}} + 5194) \times 10^{-6}. \tag{6}$$

Equation (6) is used for calculating the effective value of C_{OUT} in (4).

B. Sleeping Times

As shown in Fig. 3, the MCU goes to sleep mode (LPM) at various stages of the workflow for various amounts of times. Most of their values (t_1, t_2, t_3, t_5) are application specific and depend on available energy, load power requirement, period of load pulse etc.

Time t_4 is calculated based on the time constant of the RC network formed by R_{REF} and C_{REF}. To give enough margin, we chose t_4 as twice this time constant in our design:

$$t_4 = 2 \times R_{\text{REF}} C_{\text{REF}}. \tag{7}$$

The period of the load pulse is given by

$$T = t_2 + t_3 + t_4 + t_5. \tag{8}$$

Note from Fig. 3 that T remains the same irrespective of whether the system is in FOCV MPPT mode or MCU-assisted MPPT mode. For better MPPT accuracy, we could split t_3

into multiple parts and/or eliminate t_5 completely in order to have multiple MPP update cycles within one load pulse period. However, we must trade any gains against the increased energy consumption that will result.

As an example, the values used in the experimental validation of this work are t_1 = 1 s, t_2 = 1 s, t_3 = 10 s, t_4 = 200 ms, and t_5 = 4.8 s.

C. Harvester Capacity

A minimum average power required from the harvester can be calculated for the bare minimum function of the system, which is to sustain the periodic sense and transmit cycle. For a known input voltage V_{IN}, the minimum average input current required from the harvester can be found as

$$I_{\text{IN,MIN}} = I_{\text{OUT,MIN}}(V_{\text{OKH}} + V_{\text{OKL}})/(2\eta V_{\text{IN}}) \tag{9}$$

with

$$I_{\text{OUT,MIN}} = C_{\text{OUT}}(V_{\text{OKH}} - V_{\text{OKL}})/T \tag{10}$$

For a meaningful implementation of the proposed MPPT method, we must avoid reaching the over-voltage limit $V_{\text{OUT,OV}}$ on the output capacitor during the fixed time interval t_3 between the two sensing of V_{CC} events. Therefore, for a known input voltage V_{IN}, the maximum average input current required from the harvester can be found as

$$I_{\text{IN,MAX}} = I_{\text{OUT,MAX}}(V_{\text{OUT,OV}} + V_{\text{OKL}})/(2\eta V_{\text{IN}}) \tag{11}$$

with

$$I_{\text{OUT,MAX}} = C_{\text{OUT}}(V_{\text{OUT,OV}} - V_{\text{OKL}})/t_3 \tag{12}$$

V. Validation

A. Example System

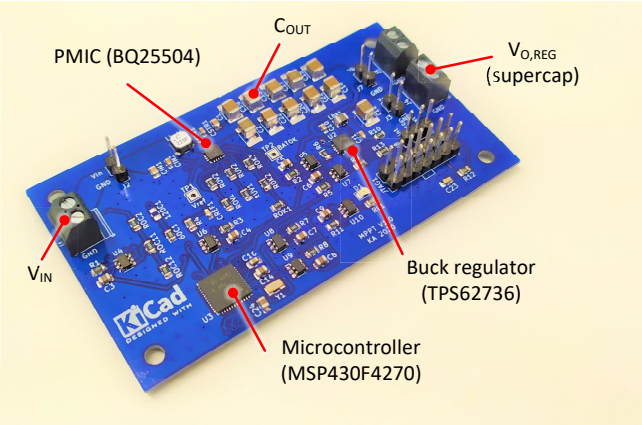

Fig. 4. Experimental setup of the proposed system.

An experimental setup as shown in Fig. 4 was built to validate the proposed concept with a 1 cm^2 PV cell (KXOB22-04X3F) used as the energy harvester. The setup uses BQ25504 [6] as the PMIC, TPS62737 as the buck regulator, and MSP430F4270 [15] as the MCU, all from Texas Instruments. The pulsed load of sense and transmit (i.e. sensor and radio respectively in Fig. 1) is emulated by a simple LED in series with a resistor after the load switch S_4. This is done to keep the system simple and focus on the MPPT part without loss of generality. A 0.33 F supercapacitor is chosen as the rechargeable storage.

The list of important components used in the experimental setup is presented in Table I. An effort was made to choose the components with the lowest quiescent and leakage currents.

TABLE I
List of Important Components

Component	Part number
PMIC	BQ25504
Buck regulator	TPS62737
MCU	MSP430F4270
AND gate	2 × TPS22860 in series
OR gate	2 × TPS22860 in parallel
S_2, S_3, S_4 (SPST switch)	TPS22860
S_1 (SPDT switch)	TMUX1119
C_{OUT}	10 × AMK432BJ477MM in parallel
Rechargeable storage	SCMR14L334SSBB0 (0.33 F supercapacitor)

B. Experimental Results

Fig. 5 shows the key waveforms of operation with the convergence of MPPT and the slow charging of the supercapacitor. The FOCV MPPT which is an inbuilt feature of the BQ25504 PMIC is visible briefly in Fig. 5, and with more details in Fig. 6. Two notable load events (sense & transmit, and buck regulator ON) are captured in Fig. 7.

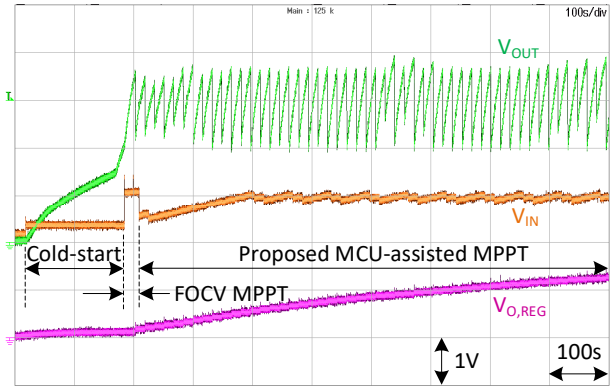

Fig. 5. Key experimental waveforms showing different stages of MPPT and slow charging of the supercapacitor.

A fixed step size of 50 mV is used for the P&O algorithm, which can be smaller or variable for better tracking. Also, the initial guess of the input voltage reference is chosen arbitrarily as 0.5 V. In practice, with prior knowledge of the harvester cell type (e.g. PV cell or TEG etc.) and rating, one can choose this initial guess more precisely to expedite the MPPT convergence.

C. Power Overhead

Table II lists the energy required to implement the proposed MPPT method [15]. Since the cycle repeats every 16 s the

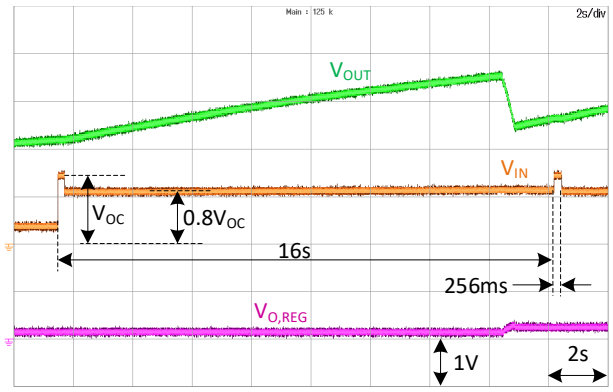

Fig. 6. Zoomed view of the FOCV MPPT algorithm integrated in the BQ25504 PMIC.

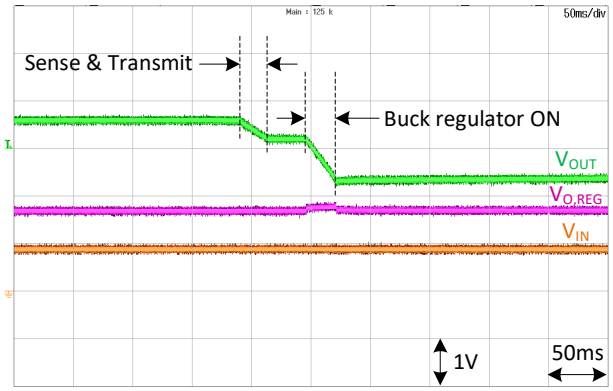

Fig. 7. Important events at each load cycle (zoomed).

average power required = 8.6 × 10^4 nJ /16s ≈ 5 μW. Added to that is the continuous power loss of about 3 V × 1 μA = 3 μW due to the leakage/quiescent currents (assumed as 1 μA) in the additional MPPT circuitry (S_1, S_2). Therefore, a total of 8 μW of power overhead is needed to implement the proposed MPPT method. In comparison, the BQ25504 has a preset 256 ms FOCV sampling period that is repeated every 16 s [18], which means it wastes 500 μW × 0.256/16 = 8 μW of power for harvesting energy from a cell with 500 μW average power.

In this example, the proposed method and the FOCV method have similar effective power consumption figures. The proposed method will produce a net energy gain if the harvester average power is larger than 500 μW, and/or if the MPP of the harvester is not well represented by a fixed open-circuit voltage.

TABLE II
ENERGY REQUIRED TO IMPLEMENT MCU-ASSISTED MPPT

Task	Time	Energy required
Sense V_{OUT} twice and calculate V_{MPP}	95 ms	$3V \times 0.3mA \times 95ms$ = 8.5 × 10^4 nJ
Charge C_{REF} (=10 nF) to V_{MPP} (=1 V, say)	5 ms	$0.5 \times 10nF \times (1V)^2$ = 5 nJ
DAC module active	5 ms	$3V \times 0.05mA \times 5ms$ = 750 nJ

VI. CONCLUSIONS

A COTS component-based dynamic MPPT method for low power energy harvesting WSN applications is demonstrated in this paper. With minimum extra components and less than 10 μW power overhead, the proposed method overcomes the shortcomings of FOCV method in the low-milliwatt power realm and does not require additional current and voltage sensors. The analysis and experimental demonstration indicate the speed and accuracy of MPPT can be traded against power consumption by adjusting the step size and the frequency of the MPPT cycle.

REFERENCES

[1] D. Newell and M. Duffy, "Review of power conversion and energy management for low-power, low-voltage energy harvesting powered wireless sensors," *IEEE Trans. Power Electron.*, vol. 34, no. 10, pp. 9794–9805, Oct 2019.

[2] Z. J. Chew, T. Ruan, and M. Zhu, "Power management circuit for wireless sensor nodes powered by energy harvesting: On the synergy of harvester and load," *IEEE Trans. Power Electron.*, vol. 34, no. 9, pp. 8671–8681, Sep. 2019.

[3] H. Abu-Rub, M. Malinowski, and K. Al-Haddad, *Power electronics for renewable energy systems, transportation and industrial applications*. John Wiley & Sons, 2014.

[4] B. Liu, S. Duan, F. Liu, and P. Xu, "Analysis and improvement of maximum power point tracking algorithm based on incremental conductance method for photovoltaic array," in *2007 7th International Conference on Power Electronics and Drive Systems*, Nov 2007, pp. 637–641.

[5] "LTC3105: 400mA step-up dc/dc converter with maximum power point control and 250mV start-up," *Linear Technology*, 2010.

[6] "BQ25504: ultra low-power boost converter with battery management for energy harvester applications," *Texas Instruments*, June 2015.

[7] "BQ25570: nano power boost charger and buck converter for energy harvester powered applications," *Texas Instruments*, Dec 2018.

[8] "SPV1050: ultralow power energy harvester and battery charger," *STMicroelectronics*, May 2018.

[9] W. Swiegers and J. H. R. Enslin, "An integrated maximum power point tracker for photovoltaic panels," in *IEEE International Symposium on Industrial Electronics. Proceedings. ISIE'98 (Cat. No.98TH8357)*, vol. 1, July 1998, pp. 40–44 vol.1.

[10] D. P. Hohm and M. E. Ropp, "Comparative study of maximum power point tracking algorithms using an experimental, programmable, maximum power point tracking test bed," in *Conference Record of the Twenty-Eighth IEEE Photovoltaic Specialists Conference - 2000 (Cat. No.00CH37036)*, Sept 2000, pp. 1699–1702.

[11] N. Femia, G. Petrone, G. Spagnuolo, and M. Vitelli, "Optimization of perturb and observe maximum power point tracking method," *IEEE Trans. Power Electron.*, vol. 20, no. 4, pp. 963–973, July 2005.

[12] S. Liu and R. A. Dougal, "Dynamic multiphysics model for solar array," *IEEE Trans. Energy Conv.*, vol. 17, no. 2, pp. 285–294, June 2002.

[13] "CC430 family user's guide," *Texas Instruments*, Jan 2013.

[14] K. Ali and D. J. Rogers, "An orientation-independent multi-input energy harvesting wireless sensor node," *IEEE Trans. Ind. Electron.*, vol. 68, no. 2, pp. 1665–1674, 2021.

[15] "MSP430x4xx: family user's guide," *Texas Instruments*, April 2013.

[16] B. Ivey, R. Hegde, and A. Bhat, "AN1267: extreme low-power (XLP) PIC microcontrollers: An introduction to microchip's low-power devices," *Microchip Technology Inc.*, July 2016.

[17] "Capacitance and dissipation factor measurement of chip multilayer ceramic capacitors," *Murata Mfg. Co. Ltd.*, Oct 2006.

[18] U. Lyles and Y. Ramadass, "BQ25504 optimization of mppt algorithm," *Texas Instruments*, Mar 2012.